2020-01-24

Tributary-junction alluvial fan response to an ENSO rainfall event in the El Huasco watershed, northern Chile

Cabre, A

10.1177/0309133319898994
Progress in Physical Geography: Earth and Environment
SAGE Publications

Paper submitted to Progress In Physical Geography

Tributary-junction alluvial fan response to an ENSO rainfall event in the El Huasco watershed, northern Chile

Albert Cabre´, Universidad Cato´lica del Norte, Chile
German Aguilar, Universidad de Chile, Chile
Anne E. Mather, Plymouth University, UK
Victor Fredes, Universidad de Chile, Chile
Rodrigo Riquelme, Universidad Cato´lica del Norte, Chile

Abstract

Tributary-junction alluvial fans situated at the intersection of confined valleys with <100 km^2 tributary catchments are of special interest to evaluate the heterogeneous consequences of extreme rainfall events in arid zones. These fans record the episodic sedimentological behaviour of the hillslope response to rainstorm events within tributary catchments, together with the influence on the main fluvial systems. In this paper, we benefit from the March 2015 event (23–26 March 2015), which produced 75–46 mm of precipitation over four days in the southern portion of the Atacama Desert. This storm event triggered several debris flows in El Huasco River watershed tributaries and, therefore, tributary-junction alluvial fans received a total of *106 m^3 of sediments across 49 activated catchments. We find that the characteristic storm signature across the catchments can be synthetised in a conceptual fan formation model based on field mapping of facies (F1 to F6) present in the fans. The characteristic signature is a record of initially high sediment-to-water flows restricted to the fan environments (mainly debris flows) followed by later, more dilute (mainly hyper-concentrated to fluvial) flows that incise the tributary-junction alluvial fan deposits and link tributary catchments with the main river. These later-stage flood event deposits, locally, are capable of ponding and compartmentalising the main river where the longitudinal connectivity of the tributary-junction catchment is effective. This situation improves tributary-junction fan slope and main-trunk-channel linkages. This approach provides a reference framework for understanding the distribution and routing of effective runoff from similar rainfall events that control the aggradation and incision of the fluvial system, which is of great value when studying past stratigraphic arrangements in these arid alleys.

I Introduction

The sedimentary processes that control alluvial fan formation have been widely studied in many environments (Blair, 1999; Blair and McPherson, 1994, 2009; Blissenbach, 1954; De Haas et al., 2014; Hartley et al., 2005; Mather et al., 2000; Stokes and Mather, 2015; Wang et al., 2008; Wells and Harvey, 1987). Within alluvial fan studies, tributary-junction alluvial fans, although they occur within a variety of mountain range settings (e.g. Al-Farraj and Harvey, 2005; Best, 1986; Bull, 1979; Crosta and Frattini, 2004; Go´mez-Villar et al., 2006; Harvey, 2002; Hooke, 2003; Mather and Stokes, 2017; Sorriso-Valvo et al. 1998; Stokes and Mather, 2015; Wang et al. 2008), have received less attention. Yet, it is clear from existing studies that the alluvial records of tributary-junction alluvial fans and related sediments provide significant potential that can be applied to further understanding of palaeoenvironmental studies, long-term dynamics of hillslope-river (dis)connectivity (Blissenbach, 1954; Colombo, 2005; Hugget, 2007; Larson et al., 2015; Lisenby and Fryirs, 2017; Mather et al., 2017) and debrisflow landslide hazards in such settings.

The infilling evolution of the arid rivers that drain the western slope of the Andes after the Last Glacial Maximum have been studied by Riquelme et al. (2011) for El Turbio (watershed adjacent to the Huasco) and Cabre´ et al. (2017) for El Tra´nsito River (tributary of the El Huasco river). These studies highlight the importance of tributary-junction alluvial fans in the valley during the Holocene as one of the greatest lateral sedimentary inputs that control the longitudinal aggradation of these valleys. The geochronological data presented in Cabre´ et al. (2017) for El Tra´nsito River imply that the main river valley was infilled by alluvial sediment continuously from *11 ka and lasted till *2 ka.

The Holocene climatic variability (from humid to more arid periods) might explain the differences in the sedimentary record in the fans. An enhanced effect of westerlies (moisture that comes from the south-west) in the early to the mid-Holocene provided the sediments needed to impede the main rivers and, thus, allow the formation of shallow water lakes where vegetation was established. Relatively more arid periods in the mid-Holocene (e.g. within 8 ka BP to *4 ka BP) (Grosjean et al., 1997, 2007; Ortega et al., 2012; Tiner et al., 2018; Tully et al., 2019) would have provided the necessary conditions to form and preserve regolith in inter-storm periods, and the shortlived rains would have been responsible for presenting similar stratigraphic arrangements to the observed March 2015 event. Spatially and temporally, distribution of these records suggests that the El Nin˜o Southern Oscillation (ENSO) signature and its temporal

variability may account for the landscape evolution of these valleys during the Holocene (e.g. Ortega et al., 2012).

Here, we explore the response of tributaryjunction alluvial fans to an extreme storm rainfall event and how these events can develop hillslope-river (dis)connectivity within a rainstorm event (e.g. Bracken et al., 2015; Fryirs, 2013; Joyce et al., 2018). (Dis)connectivity within catchments dictates the sediment yield to alluvial fans from their transport-limited catchments. The latter strongly depends on the temporal scales of the effective mechanisms (e.g. extreme storm events) (Bracken et al., 2015; Harvey, 2001, 2002; Wohl, 2017). The March 2015 event provides an excellent opportunity to understand how facies types and stratigraphic arrangements between them can condition the coupling status of alluvial fans and main rivers. Thus, the changes in (dis)connectivity in this paper are discussed for the coupling of (a) catchment hillslope-alluviated channels and (b) alluvial fans and the trunk valley. Differences in fan morphology and facies are presented to understand the impact of extreme storm events in fluvial valleys of the southernmost Atacama Desert.

II Study area background and the 23-26 March 2015 event

The study area is situated in the El Huasco River watershed. This watershed of *9850 km^2 has two main valleys (El Carmen River and El Tra´nsito River) converging at the Alto del Carmen town junction (Figure 1). El Huasco River watershed is situated at *29S in the southernmost part of the Atacama Desert where the precipitation usually occurs during southernhemisphere winters by the influence of the westerlies that supply snow above *3000 m above sea level (a.s.l.). The mean annual precipitation varies strongly with altitude, but for this study area, it is usually 200 mm/year (Salas et al., 2016). In the spring season, the melt of snow provides a progressive erosion observed in the stream sediment capture gauges (Pepin et al., 2010). Salas et al. (2016) indicated that the hydrological dynamics for the El Huasco River watershed are altered during the El Nin˜o years of the ENSO and are increasing and extending precipitation into the area. In that sense, Salas et al. (2016) presented a few above-mean precipitation events associated with El Nin˜o in the study area in the years 1955/1965, 1972/ 1973, 1987/1988, 1997/1998 and 2002/2003, and included the March 2015 event. Those events probably provided the necessary rainfall to trigger debris flows responsible for the formation of the tributary-junction fans in the past (Aguilar et al., 2014).

The Huasco River valley is one of the most studied valleys in the western slope of the Andes in terms of its geomorphological and sedimentological evolution (Aguilar, 2010; Aguilar et al., 2014; Cabre´ et al., 2017). Narrow valleys, such as the El Huasco River valley, allow streams to trim tributary alluvial fans depending on the position of the river in the floodplain (e.g. Stokes and Mather, 2015). This trimming ('toecutting' of Leeder and Mack, 2001) foreshortens the fan, mimicking a drop in base level at the new trim-line up-fan, leading to the development of new depositional 'healing lobes' (Colombo, 2010; Giles et al., 2016; Leeder and Mack, 2001; Mather et al., 2017) below the new termination, giving a telescopic-like shape (Colombo, 2005, 2010).

The March 2015 event triggered erosion in the catchments of the Huasco River watershed represented by (a) rills and gullies (dependent on catchment slope colluvial or regolith properties) and (b) bedload erosion of sediments in the alluviated channels of the catchments (online appendix: Figure A1).

III Methods

1 Field survey and volume calculations

Two weeks after the March 2015 event, fieldwork observations and measurements were carried out in El Huasco River valley. The initial observations of the landscape changes prior to engineering works allowed us to map and sample the debris flows that reached the valley floor and modified the previous fan surfaces and channel junctions. Forty-nine fans were selected that presented debris flows generated in the March 2015 event (online appendix: Table A1). Mapping was undertaken using the available imagery from Google Earth (5 m resolution) and RapidEye (5 m resolution) provided by the Advanced Mining Technology Center, together with a specialised aerial survey using a DJITM Phantom 3 quadcopter. The volume calculations for the 49 debris-flow deposits from the March 2015 event, which use the field measurements of the depositional and erosional features, were presented in Aguilar et al. (2019). Their equation calculated the volume of fans by assuming a simplistic conical geometry and was adapted from the Campbell and Church (2003) equation for colluvial fan volume calculations:

$$V = \left(\frac{wlt}{2}\right)\frac{\pi}{3} \qquad (1)$$

Width (w) and thickness (t) of fan toes were measured in the field with a measuring tape for 16 alluvial fans, whereas their axial length (l) was measured on the RapidEye imagery. Width and length for the rest of the fans (33) were measured from RapidEye images. In these cases, we

estimated 1 m of event-sediment thickness, on average, for each fan based on mean field observations. The volumes have been corrected with a bulking factor, which considers a porosity value of 30% (Nicoletti and Sorriso-Valvo,1991). The resulting fans after the March 2015 event were classified based on the sediment volumes accumulated from the storm based on Jakob's (2005) threshold values (Figure 2). Type A corresponds to $<10^3$ m^3 sediment volumes; type B corresponds to between 10^3 and 10^4 m^3; and type C to volumes $>10^4$ m^3. The calculated volumes (online appendix: Table A1) represent minimum values because there was a sediment loss due to the immediate river erosion after aggradation onto the floodplain and due to the erosional processes in the fan.Facies types were identified using grain/clast shape, textural parameters, relief and stratification type. Particle-size measurements of thelargest clasts were done in the field to obtain their mean diameter by sampling oriented photographs covering 360 cm^2 to assess grain size for each facies type (Ibbeken and Schleyer, 1986; Wells and Harvey, 1987). Finally, the granulometric distributions for eight samples were obtained from standard sieving tests at the laboratories of Universidad Cato´lica del Norte in Antofagasta, Chile.

2 Catchment morphology

We studied 124 tributary catchments that drain into El Carmen and El Tra´nsito rivers, including the 49 selected for the detailed study of tributary-junction alluvial fans (Figure 3). The tributary catchments were extracted from a Digital Elevation Model with a nominal spatial pixel resolution of *30 m 30 m (https://aster web.jpl.nasa.gov/gdem.asp) and a nominal vertical resolution of 1.0 m using QGIS Geographic Information System (https://qgis.org/es/site/). Morphometric and hydrological features of tributary catchments were selected to analyse their influence on the tributary-junction alluvial fans. The catchments were evaluated for five attributes likely to influence peak flow generation, sediment production and hydrological conditions (Stokes and Mather, 2015; Wells and Harvey, 1987; Wilford et al., 2004): catchment area (km^2); catchment length (km), measured from the highest points of the catchments towards the exhutories as a straight line; catchment gradient (km/km), the division of catchment relief by catchment length; catchment relief (m), which considers the difference in altitude between the lowest and highest points of the tributary catchment; and catchment drainage density (km/km^2) (online appendix: Figure A2, Tables A1, A2).

3 Catchment geology

Five geological groups (Geo 1 to Geo 5) were defined to assess the influence of rock units upon sediment generation for the mass flows based on the geological units presented in Salazar et al. (2013) (Figure 3). These groups document the geotechnical values of strength (S), cohesion (C) and porosity (P) (Gonza´lez de Vallejo et al., 2002) (online appendix: Figure A3). The classification represents an approximation of the geotechnical conditions of the watershed bedrock in the zone that, from the literature, is considered as a first-order approach to forecast grain size and feasibility to form a regolith (e.g. Roda-Boluda et al., 2018). The percentage of the watershed area encompassed by each geological group was then calculated (Figure 3). A map of mantled hillslopes (either colluvium or regolith) is presented in (Figure 3), overlying the geological units of Salazar et al. (2013) to assist in identifying sediment source areas for the March 2015 event. The sedimentology of the deposits is described in more details in Aguilar (2010) and Cabre´ et al. (2017).

IV Results

1 Catchment characteristics

1.1 Morphology. The tributary catchments that were activated after the March 2015 event range from 128 to 0.23 km^2, relief varies from 2730 to 1060 m, catchment length ranges from 16.75 to 0.93 km, gradients vary from 0.73 to 0.13 and drainage densities vary from 2.5 to 6 (online appendix: Table A3, Figure A2). Most of the tributary catchments of El Carmen River are routed east–west, whilst the ones that drain into El Tra´nsito River are related more closely to a north–south trend on average (Figure 2).

1.2 Geology. The five geological groups defined to assess the influence of rock units upon sediment generation for the mass flows highlight differences between fan responses (type A, B and C based on volume; from Jakob, 2005). Figure 3 summarises the presence of geological groups (Geo 1 to Geo 5) depending on volume-based fan type (A, B, C or catchments with no sediment discharge in the March 2015 event). Valley-floor-infilling sediments of the trunk valleys were not considered as they do not contribute to sediment transfer from the catc ments to the tributary-junction fans.

2 Fan response

The flood event sedimentology and spatial and temporal distribution of the facies in the tributary-junction alluvial fans after the rainfall are described here. The facies include cohesive debris flows (F1), dilute debris flows (F2), cohesionless debris flows (F3), transitional flows (F4),

sheet floods (F5) and ponded deposits (F6). The flood event chronology is presented as a conceptual model that summarises the fan response to the March 2015 event.

V Flood event sedimentology

1 Facies 1 (F1)

1.1 Description. Facies 1 is represented by lobes of sediment with variable widths (1 to >100 m) on the size of the depositional area available on the pre-existent alluvial fan surfaces. Thickness of the deposits ranges between 30 and 100 cm. The surface of these lobes present undulations (pressure ridges) showing strips with an oriented clast fabric parallel to the lobe front and are mainly matrix-free (Figure 4(a)–(c)). The strip or bands are best illustrated in Figure 4(c). The pressure ridges on the lobe fronts include boulder accumulations interlocked in the frontal lobe. Additionally, facies 1 present levees on the sides of the channel that can be observed along the fan (online appendix: Figure A4).

Facies 1 consists of unsorted clast-rich fractions, which contain boulder-sized clasts with bmax of >70 cm and the fabric present in these facies varies from clast-supported to matrixsupported. The coarse fraction ranges from 10 to 60 mm. In vertical sections in the stratigraphy of these facies, there is a predominance of matrix-supported clasts (Figure 4(a)–(b)) with poorly sorted pebble and cobble gravels. Grain-size analysis (Figure 5) was performed on the matrix of these deposits (P2MSS-01, C1MSS-01 and C1MSS-03) collected at stations close to the fan apex area (online

appendix: Figure A5(a), (b)). The matrices of these facies are composed of pebbles through to sands, from very coarse to fine sand, and minor silt and mud (<5%) (Figure 5).

1.2 Interpretation. Facies 1 are the result of cohesive debris flows (Wells and Harvey, 1987). These facies are present in the apex area and the mid-portion of the fans, and their surface expression is controlled by the prior topography. The loss of confinement as soon as the flow exits the tributary valley is responsible for the expansion on the apex area of the fans and usually corresponds to the higher surfaces of the fans. These facies are the result of a highly cohesive flow supported by the high density and strength of the mass (Blair and McPherson, 2009; Costa, 1984; Wells and Harvey, 1987) from a single pulse of sediment that corresponds to the first stages of the sediment arriving at the alluvial fans, with low water:sediment ratio. The loss of confinement of flows, the loss of the water content out of the margins of the flows and via infiltration, and the change of slope led to the deposition of this facies on the uppermost portion of the fans in levees and lobes.

2 Facies 2 (F2)

2.1 Description. Facies 2 appears as narrow lobes, with the thickness of the deposits ranging between <10 and 30 cm. The surface of this facies comprises a lobate shape that corresponds to multiple sediment pulses. The lobes are narrow with length:width ratio typically between 1 and 4, and are usually vertically stacked (Figure 4(d)–(f)). These facies also present polygonal desiccation mud-crack morphologies on the surface (Figure 4(e)).

Facies 2 consists of gravels with cobbles (b-max of 15 cm), pebbles, granules and sands with a matrix-supported fabric. Grain-size analysis was performed on the matrix of these deposits of stations ranging from the apex area to the midportion of the fan depending on the fan type (Figure 5). The matrix includes silty muds up to 5–12% and granule accumulations of this facies that present clast-supported fabric (Figure 4(e)). Stratification is lacking for these facies and in some field examples includes orientated plant remains on the top of the deposits that indicate the flow direction (Figure 4(e)).

2.2 Interpretation. Facies 2 represent dilute debris flows similar to the transitional debris flows in the study by Wells and Harvey (1987). These facies are present in the apex area and the midportion of the fans. Their spatial extent is controlled by the topography that is usually related to facies 1 from the same event. Facies 2 present several lobes due to the different debris-flow surges from the apex area during the event (Figure 4(f)). There are two possible interpretations about the origin of these facies, depending

on the fan area where we find facies 2. The transient behaviour of these facies within cohesive but more diluted facies is related to a higher water:sediment ratio. Thus, these facies might reflect a lack of sediment available to be transported from the tributary catchment due to initial sediment flushing by the initial cohesive flows (F1). Local variations in precipitation intensity combined with linkage between partial area contributions through the storm could influence the total amount of surface runoff availability in the catchment channel (Mather, 2006). The morphology of these multi-lobe facies is related to multiple surges during the rainstorm event. In some fans, it is evident that F2 may be locally derived from F1 deposits in distal locations due to re-working by subsequent flows.

3 Facies 3 (F3)

3.1 Description. Facies 3 appear as arcuate push ridges and longitudinal lobate bars that only occur in the active depositional lobes (Figure 4(g)–(i)). Longitudinal bars are present in the feeder channel of the alluvial fans and the arcuate push ridges in the proximal active depositional lobes. Type 3 facies present moderate thicknesses ranging from 5 to 30 cm

depending on whether they are linear or lobate bar-forms. These deposits correspond to open-framework coarse sediments with clastsupported fabrics (Figure 4(g)–(i)) and a matrixfree top. These facies have low matrix content and consist mainly of clasts, with a b-max of up to300cminthechannelbedsandupto20cmin the arcuate push ridges.

3.2 Interpretation. Facies 3 are defined as cohesionless debris flows (Mather and Stokes, 2017; Postma, 1986). They are limited to the channels that distribute sediment on the fans after the storm towards the fan toe or to the new lobes on the telescopic-like alluvial fans. The arcuate shape of the flow deposits (Figure 4(h)–(i)), with openwork boulders, represents push ridges on the depositional new lobes at the fan toe as a consequence of pulses or surges observed in debris flows (Pierson, 2005; Wells and Harvey, 1987).

The presence of boulders with a b-max of 300 cm in the feeder channels may be either related to the transport processes of F1 facies, where, in later stages of the storm event, the matrix might have been washed out by the greater water:sediment ratios, or might correspond to lag deposits of prior storm events. In one fan, it is possible to identify such large boulders prior to the storm because they have F1 and F2 facies on their top.

4 Facies 4 (F4)

4.1 Description. Facies 4 comprise depositional bars with moderate depositional relief (<50 cm). These facies consist entirely of pebbles, cobbles and boulders, forming elongated shapes either in the feeder channels (Figure 4(j)–(l)) or in the lobes formed at the toe, showing a radial distribution pattern of the flows. Grain-size analysis was performed on P2MSS-03 on the scarce matrix and consists of pebbles, sands and lower percentages of silty muds (5%; Figure 5).

4.2 Interpretation. Facies 4 could be interpreted as hyper-concentrated flows (Blair and McPherson, 2009; Pierson, 2005; Wells and Harvey, 1987). These facies are interpreted as fluvial longitudinal bars associated with the removal of facies 3. The low amounts of fine sediments suggest a continuous washing of clean waters provided from the feeder catchment after the event. Many erosive features also suggest the turbulent behaviour of the flows responsible for the deposition of these facies, although many of these channels provide space to be filled with facies 5 (Figure 4(m)).

5 Facies 5 (F5)

5.1 Description. Facies 5 describe fine-grained channel-fill and sheet-like sands. These facies correspond to sand bodies and granules, which fill channels or scatter on the active depositional lobes (Figure 4(m)). The sheets vary between <1 and 2 cm in thickness and are well stratified.

Grain-size analysis was performed on P2MSS04 and shows a matrix composed of mainly medium to fine sands, with minor silt and mud (12%; Figure 5). The final stage includes some minor (<1 m) incision.

5.2 Interpretation. The presence of laminated sand sheets indicates tractional flow, and the lower amounts of fine sediments are attributed to the flushing of clean waters. In this setting, water:sediment ratios are high relative to F1, F2 and F3. Facies 5 are transported by the feeder channels towards the lower depositional lobes where they aggrade as extensive sand sheets; they also fill the fan channel. Thus, they reflect a pulse of more water-rich flows through the system, which is common after the initially available sediment has been flushed out by the earlier part of the storm (e.g. Mather and Hartley, 2005).

6 Facies 6 (F6)

6.1 Description. Facies 6 occur in the main river areas above the fans and describe fine laminated sheets present in conjunction with F5, F4 and F3 facies lobes, which impede the main river. These facies correspond to silty muds, muds and sandy sheets (Figure 4(p)–(r)). In some fans, we can recognise bird footprints (Figure 4(q)), human footprints and several anthropogenic materials such as cars are deposited together with these facies. Mud-cracks are present in these facies (Figure 4(q)–(r)). Grain-size analysis was performed on sample CRU-250315-2 and comprises mainly fine sand (40%) and silty muds (30%) (Figure 5).

6.2 Interpretation. Facies 6 are deposited above where the active depositional lobe of the tributary-junction alluvial fans dam the main river, creating ephemeral palustrine conditions. These facies contain mud-cracks that are developed on the surface when evaporation or opening of the barrier by the streamflow changes the local water-table level. Additionally, wood fragments transported by the main river or established vegetation might be found in these deposits. Similar carbon-rich layers are preserved within the Holocene stratigraphy, which may reflect a similar depositional environment (Cabre´ et al., 2017).

VI Characteristic model of flood event chronology

In order to understand the March 2015 flood event, controls on the tributary-junction alluvial fans formation, the stratigraphic and spatial relations of the facies and geomorphic features can be utilised to reconstruct the relative chronology of the depositional and erosional processes in the tributary-junction alluvial fans. Differences in facies associations can be used to understand (a) changes to the water:sediment ratio of flows; (b) the coupling degree between fans and the main river; and (c) the sedimentary characteristics of the available sediment coming from the

catchments. Detailed mapping of facies distribution has been undertaken to understand the cross-cutting relations for the six different types of facies recognised in the area (online appendix: Figure A5).

We propose a typical sequence of events for the March 2015 rainstorm based on the correlation of the different facies in the fans and the relative time of erosion and deposition during the storm (Figure 4). F1 and F2 facies types, where preserved or present, correspond to the first debris flows yielded onto the fans related to lower water:sediment flow events. A number of debris-flow surges are recorded within the different lobes of the fans. Following the deposition of F1 and F2, entrenchment of the main tributary channel, associated with more fluid transitional flows, occurred. These flows range from cohesionless debris to hyper-concentrated, and are recorded by F3 deposits. After this phase, more dilute flows erode the previously deposited materials and enable the deposition of F4 and F5 facies further downstream (online appendix: Figure A6). The local river baselevel is reached after this incision (e.g. online appendix: Figure A5(b)). New telescopic-like fans are then formed with open-framework
boulders and lobate gravel lenses. Later flows are even more diluted and transport the fines downstream, resulting in openframework gravel deposits, evidenced downflow by pools of fine sediments within F3 and F4 facies (Figure 4(g)).

Facies 6 are always related to the presence of a new lobe formed in the main valley that enables damming of the main river and forms an ephemeral palustrine environment upstream. The facies present in the new lobes vary between fans with F3, F4 and F5.
This characteristic conceptual model of tributary-junction alluvial fan behaviours in this arid zone, based on the facies assemblages and the erosional features, provides the first such example from the Andes mountain range.

VII Discussion

As a first-order approach, differences in facies types on alluvial fans are attributed to differences in the relative fluidity of the flows primarily controlled by the amount of water (Wells and Harvey, 1987). However, the lack of meteorological stations across the study area of La Sierra del Medio (some in 100 km^2) means that any significant spatial variation in rainfall distribution and intensity cannot be directly assessed. However, by examining the relationship between the flood event chronology and resulting facies, we can gauge the relative influence of catchment

morphometrics, geology and flow deposits, and assess the relative importance of these variables to the resulting facies types.
Additionally, consideration of the lateral (slope-channel) and longitudinal (along valley) tributary catchment connectivity (Bracken et al., 2015; Fuller and Massey, 2011; Harvey, 2002; Mather and Stokes, 2017; Wohl, 2017) can assist in explaining the sediment volumes removed from the tributary catchments that were delivered to the tributary fans and interacted with the main rivers during the March 2015 event.

1 Controls on (dis)connectivity of catchments
The sediment transference from catchment to fans occurs in floods of sufficient magnitude to reach and exceed the catchment mouth (Mather and Stokes, 2017; Stokes and Mather, 2015). Thus, sediment deposition in the fans is controlled, to a large extent, by the longitudinal (along tributary valley) connectivity that is favoured by extreme storms (e.g. March 2015 event) in transport-limited catchments associated with arid environments. Sediment transport is typically minor during smaller, inter-storm periods, preventing sediment discharge reaching the fans. While the influence of the differential adjustment of sediments inside the catchments is controlled by the connectivity, it is, in turn, strongly dependent on the selected morphometrics (online appendix: Table A1).

From the analysis of the selected morphometrics, we observe an inverse relationship between the sediment discharge and relief. This suggests that the relief is strongly dependent on the catchment size, whereas the discharge of sediments follows a power law where greater sediment discharge depends on the catchment gradient (online appendix: Figure A7). This suggests that greater effectiveness in connectivity permits the stored sediments in the mantled hillslopes to be removed from small and steep catchments during individual events such as the March 2015 event (supplementary Figure A7(a)). In contrast, larger and gentler catchments store sediment in local aggradation zones that inhibit the transmission of sediments down-system (Harvey, 2001; Stokes and Mather, 2015), as shown in supplementary Figure A7(b), resulting in smaller sediment discharge in the fans relative to the catchment area. This trend can be distinguished in type A and type B fans. The number of type C fans evaluated appears to be insufficient to identify any such trend.

Within-catchment lithological differences can play an important role by determining the amount and size of sediment available for transport by a rainstorm event (Mather and Stokes, 2017 and

references therein). The presence of different facies in the fans based on granulometry suggests that the available grain sizes exported from the catchments vary depending on the transport processes, lithology, structure (discontinuity spacing; e.g. bedding thickness, joint spacing) and weathering (e.g. RodaBoluda et al., 2018). Thus, the use of rockstrength values for the rock units presented in La Sierra del Medio can be an indicator of differences in the spatial variability of accumulations of regolith (Figure 3). In that sense, regolith production depends on the weathering resistance (both physical and chemical) of the Geo units, which finally controls the colluvium storage in the hillslopes. The weathering rates depend on landscape stability and climate (Carretier et al., 2018). Thus, under more humid climate conditions in the study area – for example, during the late Pleistocene (Aguilar, 2010; Cabre´ et al., 2017; Veit, 1996) – the weathering rates might have been enhanced (Riebe et al., 2004, 2015) and primed the necessary sediment storage to became transport-limited catchments during the Holocene; whereas, in more arid periods, stability in catchments might lead to greater accumulations of sediments in the alluviated channels available to be transported, suggesting a shift from weathering-limited-like catchments to transport-limited catchments typical of arid zones.

However, morphometrics and geology's role in this area might be masked by (along-valley) connectivity when we consider the longitudinal connectivity as an indicator of the effectiveness in delivering sediment to the tributary-junction alluvial fans from the catchments, as seen in Mather and Stokes (2017) in arid catchments of Morocco. In that sense, geology and morphometrics do not appear to explain the distribution of active and inactive catchments (Figure 3 and supplementary Figure A2). Hence, we have evaluated the area of mantled hillslopes against the volumes deposited in the tributary-junction alluvial fans considering that the net sediment storage is the dominant signature in the transport-limited catchments that characterise arid zones (e.g. Bovis and Jakob, 1999). Such catchments are typified by large areas of mantled hillslopes and alluvial sediments filling the channel network.

The results suggest a clear control of volume yielded against the percentage of mantled hillslopes per catchment (online appendix: Figure A8). Thus, a power law where watershed areal coverage of sediments (either colluvium or regolith) define a cluster of Type A or Type B fans can be proposed. For Type C fans, no cluster can be observed, possibly due to the lower connectivity within larger catchments that is supported by the presence of sedimentation zones (sediment storage areas) within these catchments, as suggested by Mather and Stokes (2017).

This would imply that the sediments deposited in the type C fans mainly come from the alluviated channels.

Finally, the March 2015 event has shown that even the small catchments (<5 km^2), with 10% of sediment-mantled areas, are prone to deliver sediments to the outlets during an individual rain event. This appears to overcome the hazardous potential that is usually attributed to bigger catchments responsible for more dilute hazardous events.

The unusual higher elevation of the zero isotherm after the March 2015 event (summer season) could account for later pulses of sediment, as described in Moreiras et al. (2018) for the Argentinean Andes during a similar event. This is especially true for catchments with large areas above 3000 m a.s.l., where snow is typically present during winter storms. Typically, snow cover inhibits surface runoff until it melts in the southern hemisphere spring season, but snowmelt might produce F3 and F5 facies by washing out the fine sediments present in the channels. Thus, increasing frequency of extreme El Niño events could provide the necessary transport mechanisms to gradually remove the sediment from a wide range of different catchments sizes, reliefs, lengths and drainage densities.

2 Changes in (dis)connectivity as a result of an extreme storm event

The hydrological events in the study area that enable the transference of sediments are rare and have return times in the order of 100 years (e.g. Aguilar et al., 2019; Ortega et al., 2019). Thus, hillslope stability, together with thick regolith accumulations and soil production, prepare the hillslopes during interstorm periods to supply sediment for any storm that affects the area towards the channel/drainage network. The changes in (dis)connectivity after the March 2015 event are discussed and summarised in Figure 7 for (a) withincatchment hillslope sediment coupling and (b) the zonal coupling between alluvial fans and trunk valley.

2.1 Within-catchment hillslope sediment coupling.

The channel network situated within the catchments store sediments between storms. Consequently, these alluviated streams are strongly impacted by extreme hydrological events with strong incision and sediment removal downsystem. The strong erosion also induces basal erosion of mantled hillslopes situated within the catchments. This, in turn, represents an effective coupling mechanism that enhances sediment accumulation in the hill-foot zone caused by diverse landslide processes such as shallow landslides or toppling of colluvial sediments that

rapidly infill the channels (Figure 7). The effectiveness of hillslope coupling within the catchments immediately prepares 'new' available sediment in the alluviated streams to be transported during the next storm. This has been observed from field observations that in larger catchments ($A > 50$ km^2) present thicker regolith accumulations, whereas in small catchments ($A < 50$ km^2) with greater mean slope values and greater channel gradient, regolith accumulations are thinner and, thus, the effective lateral connectivity is lower. Additionally, to explain the differences in effective lateral connectivity, Stokes and Mather (2015), Lisenby and Fryirs (2017) and Mather and Stokes (2017) indicate that larger catchments might enhance sediment storage with the presence of buffers and internal barriers. Thus, the recovery period within larger catchments after an event like that of March 2015 is almost instantaneous. A summary of how effectiveness in coupling dictates the sediment routing in larger transport-limited catchments (>50 km^2) is presented in Figure 7(a).

2.2 The zonal coupling between alluvial fans and trunk valley. The coupling control mechanisms in alluvial fans are dependent on the intrinsic thresholds (e.g. fan-head trenching) and on the extrinsically controlled mechanisms (tectonic and climatic influence) (Clarke et al., 2010; Harvey, 2013). Together, extrinsic and intrinsic controls determine the coupling status of alluvial fans and, finally, the sediment bypass into the downstream fluvial, which is of major interest when evaluating the fluvial system evolution. Thus, the changes from aggradation to dissection in the alluvial fans vary from autogenic controls (e.g. Clarke et al., 2010; De Haas et al., 2016) and are determined from the changes in fan morphology by fan-head trenching, channel avulsions or lateral channel migration, whereas extrinsic mechanisms such as toe-cutting (Harvey, 2011; Larson et al., 2015; Leeder and Mack, 2001) steepen the fan channel, promoting incision in fan channels during flood events changing the sedimentation zone to the fan toe showing a telescopic-like shape (e.g. Colombo, 2005, 2010; Colombo et al., 2000).

The extreme storm event of March 2015 strongly impacted the coupling status in the tributary-junction alluvial fans, promoting severe incision in fan channels and aggradation in the trunk valley, damming large areas upstream (Figure 7(b)). The shift of the coupling status of tributary-junction alluvial fans from buffers to couplers allows transmission of sediment down-system, which is of primary interest when evaluating fluvial system geomorphological evolution during the Holocene. A summary of fan morphology changes is presented in Figure 7(b), based on the coupling status and mechanisms of an extraordinarily well-preserved tributary-junction alluvial

fan. The non-coupled status of tributary-junction alluvial fans caused debris-flow sedimentation on the alluvial fan surfaces. This has been observed in ephemeral valleys, valleys with low permanent runoff and in valleys where the March 2015 event did not significantly increase the peak flow. Differences in partially to totally coupled tributary-junction alluvial fans are derived from differences in the sediment-towater ratio of facies, topographical attributes of alluvial fans (local gradient and mean slope) and to basally induced mechanisms depending on the alluvial fan-trunk valley interactions.

3 Significance for interpreting Holocene records

The nature of the geomorphic evolution during one extraordinary rainstorm event (e.g. March 2015 event) shows how these fans are formed and degraded within an individual event, underscoring the challenges involved in understanding the longer-term record (e.g. Kain et al., 2018; Mather and Hartley, 2005; Mather and Stokes, 2017). The appreciation of the characteristic behaviour during a single event better informs our understanding of the past dynamics for such arid river systems and provides a sedimentary approach in the alluvial fan environment for recognising the increase of El Nin˜o influence described in lacustrine and fluvial environments for the last 2 ka BP (Aguilar, 2010; Cabre´ et al., 2017; Kock et al., 2019; Martel-Cea et al., 2016, Tiner et al., 2018).

The facies preservation on the late Holocene stratigraphic record might be compromised during the increase of El Nin˜o influence, as seen in the ‘cannibalising behaviour’ of the tributaryjunction alluvial fans during a single event. This suggests that the stratigraphy of tributaryjunction alluvial fans may not fully preserve the increase of the El Nin˜o influence that is recorded in closed-sedimentary systems such as peatlands and lakes during the late Holocene (e.g. Tiner et al., 2018).

VIII Conclusions

This study presents the analysis of tributaryjunction alluvial fan response and coupling status to an intense El Nin˜o rainstorm (March 2015 event) in an arid Andean watershed situated in the southern Atacama Desert. The resulting facies assemblage is the first empirical example of a typical sequence for an El Nin˜o rainstorm event described in the Andes. The dynamics of the evolving sedimentary flow rheologies (five facies characterised) through the rainfall event provide important insights into the resulting sedimentary signature of such rainstorm events that can be used to aid interpretation of the paleo-record and landslide hazard assessment. These

findings suggest that the catchment response and sediment volumes are broadly controlled by the connectivity of the catchments. The differences in sedimentology highlight a strong reliance on the nature of (dis)connectivity within tributary catchments and between the tributary-junction alluvial fans and the main trunk rivers. The ENSO signature on the alluvial fans favours (dis)connectivity and flushing of stored sediments in those catchments, which has been underestimated in the Andean fluvial systems to the date.

References

Aguilar G (2010) Erosion et transport de mati`ere sur le versant occidental des Andes semiarides du Nord du Chili (27-32□S): d'une approche a` grande e´chelle temporelle et spatiale, jusqu'a` l' e´volution quaternaire d'un syst`eme fluvial. Doctoral thesis, Universite´ de Toulouse, France, 204 pp.

Aguilar G, Cabre´ A, Fredes V, et al. (2019) Erosion after an extreme storm event in an arid fluvial system of the southern Atacama Desert: An assessment of magnitude, return time, and conditioning factors of erosion caused by debris flows. Natural Hazards and Earth System Sciences. https://doi.org/10.5194/nhess-2019239.

Aguilar G, Carretier S, Regard V, et al. (2014) Grain sizedependent ^{10}Be concentrations in alluvial stream sediment of the Huasco Valley, a semi-arid Andes region. Quaternary Geochronology 19: 163–172.

Al-Farraj A and Harvey AM (2005) Morphometry and depositional style of Late Pleistocene alluvial fans: Wadi Al-Bih, northern UAE and Oman. In: Harvey AM, Mather AE and Stokes M (eds) Alluvial Fans: Geomorphology, Sedimentology, Dynamics. London: Geological Society of London, Special Publications, 251, 85–94.

Best JL (1986) The morphology of river channel confluences. Progress in Physical Geography 10: 157–174.

Blair T (1999) Sedimentology of the debris-flowdominated Warm Spring Canyon alluvial fan, Death Valley, California. Sedimentology 46: 941–965.

Blair TC and McPherson JG (1994) Alluvial fans and their natural distinction from rivers based on morphology, hydraulic processes, sedimentary processes, and facies assemblages. Journal of Sedimentary Research 64A: 450–489.

Blair TC and McPherson JG (2009) Processes and forms of alluvial fans. In: Parsons A and Abrahams A (eds) Geomorphology of Desert Environments. Dordrecht, The Netherlands: Springer, 413–467.

Blissenbach E (1954) Geology of alluvial fans in semiarid regions. Geological Society of America Bulletin 65: 175–190.

Bovis MJ and Jakob M (1999) The role of debris supply conditions in predicting debris flow activity. Earth Surface Processes and Landforms 24: 1039–1054.

Bracken LJ, Turnbull L, Wainwright J, et al. (2015) Sediment connectivity: A framework for understanding sediment transfer at multiple scales. Earth Surface Processes and Landforms 40: 177–188.

Bull WB (1979) Threshold of critical power in streams. Geological Society of America Bulletin 90: 453–464.
Cabre´A,AguilarGandRiquelmeR(2017)Holocene evolution and geochronology of a semiarid fluvial system in the western slope of the Central Andes: AMS 14C data in El Tra´nsito River Valley, Northern Chile. Quaternary International 438(A): 20–32.
Campbell D and Church M (2003) Reconnaissance sediment budgets for Lynn Valley, British Columbia: Holocene and contemporary time scales. Canadian Journal of Earth Sciences 40: 701–713.
Carretier S, Godde´ris Y, Martinez J, et al. (2018) Colluvial deposits as a possible weathering reservoir in uplifting mountains. Earth Surface Dynamics 6: 217–237.
Clarke L, Quine TA and Nicholas A (2010) An experimental investigation of autogenic behaviour during alluvial fan evolution. Geomorphology 115: 278–285.
Colombo F (2005) Quaternary telescopic-like alluvial fans, Andean Ranges, Argentina. In: Harvey AM, Mather AE and Stokes M (eds) Alluvial Fans: Geomorphology, Sedimentology, Dynamics. London: Geological Society of London, Special Publications, 251, 69–84.
Colombo F (2010) Sedimentolog´ıa. Del proceso f´ısico a la Cuenca sedimentaria. Textos Universitarios 46. Madrid: CSIC.
Costa JE (1984) Physical geomorphology of debris flows. In: Costa JE and Fleischer PJ (eds) Developments and Applications of Geomorphology. Berlin: Springer, 268–317.
Crosta GB and Frattini P (2004) Controls on modern alluvial fan processes in the Central Alps, Northern Italy. Earth Surface Processes and Landforms 29: 267–293.
De Haas T, van den Berg W, Braat L, et al. (2016) Autogenic avulsion, channelization and backfilling dynamics of debris-flow fans. Sedimentology 63: 1596–1619.
De Haas T, Ventra D, Carbonneau PE, et al. (2014) Debrisflow dominance of alluvial fans masked by runoff reworking and weathering. Geomorphology 217: 165–181.
Fryirs K (2013) (Dis)connectivity in catchment sediment cascades: A fresh look at the sediment delivery problem. Earth Surface Processes and Landforms 38: 30–46.
Giles PT, Whitehouse BM and Karymbalis E (2016) Interactions between alluvial fans and axial rivers in Yukon, Canada and Alaska, USA. In: Ventra D and Clarke LE (eds) Geology And Geomorphology of Alluvial Fans: Terrestrial and Planetary Perspectives. London: Geological Society of London, Special Publications, 440.
Go´mez–Villar A, Alvarez-Martinez J and Garcia–Ruiz JM (2006) Factors influencing the presence or absence of tributary-junction fans in the Iberian Range, Spain. Geomorphology 81: 252–264.

Gonza´lez de Vallejo L, Ferrer M, Ortun˜o L, et al. (2002) Ingenier´ıa Geolo´gica. 1st ed. Madrid: Prentice Hall Pearson Educacio´n, 750 pp.
Grosjean M, Santoro CM, Thompson LG, et al. (2007) Climate change and cultural dynamics: A global perspective on Mid-Holocene transitions. Elsevier, 67 pp.
Grosjean M, Valero-Garce´s BL, Geyh MA, et al. (1997) Midand late-Holocene limnogeology of the Laguna del Negro Francisco, northern Chile, and its palaeoclimatic implications. The Holocene 7(2): 151–159.
Hartley AJ, Mather AE, Jolley E, et al. (2005) Climatic controls on alluvial-fan activity, coastal Cordillera, northern Chile. In: Alluvial Fans: Geomorphology, Sedimentology, Dynamics. London: Geological Society of London, Special Publications, 95–115.
Harvey AM (2001) Coupling between hillslopes and channels in upland fluvial systems: Implications for landscape sensitivity, illustrated from the Howgill Fells, northwest England. Catena 42: 225–250.
Harvey AM (2002) Effective timescales of coupling within fluvial systems. Geomorphology 44: 175–201.
Harvey AM (2011) Dryland alluvial fans. In: Thomas DSG (ed) Arid-Zone Geomorphology. 3rd ed. Chichester: Wiley-Blackwell, 333–371.
Harvey AM (2013) Processes of sediment supply to alluvial fans and debris cones. In: Schneuwly-Bollschweiler, et al. (eds) Dating Torrential Processes on Fans and Cones. Advances in Global Change Research 47.
Hewitt K (2006) Disturbance regime landscapes: mountain drainage systems interrupted by large rockslides. Progress in Physical Geography 30(3): 365–393.
Hooke JM (2003) Coarse sediment connectivity in river channel systems: A conceptual framework and methodology. Geomorphology 56: 79–94.
Hugget RJ (2007) Fundamentals of Geomorphology. Routledge Taylor and Francis Group, 483 pp.
Ibbeken H and Schleyer R (1986) Photo-sieving: A method for grain-size analysis of coarse-grained, unconsolidated bedding surfaces. Earth Surface Processes and Landforms 11: 59–77.
Jakob M (2005) A size classification for debris flows. Engineering Geology 79(3): 151–161.
Joyce HM, Hardy RJ, Warburton J, et al. (2018) Sediment continuity through the upland sediment cascade: Geomorphic response of an upland river to an extreme flood event. Geomorphology 317: 45–61.

Kain CL, Rigby EH and Mazengarb C (2018) A combined morphometric, sedimentary, GIS and modelling analysis of flooding and debris flow hazard on a composite alluvial fan, Caveside, Tasmania. Sedimentary Geology 364: 286–301.
Kock ST, Schittek K, Ma¨chtle B, et al. (2019) Late Holocene environmental changes reconstructed from stable isotope and geochemical records from a cushion plant peatland in the Chilean Central Andes (27□S). Journal of Quaternary Science 34(2): 153–164.
Larson PH, Dorn RI, Faulkner DJ, et al. (2015) Toe-cut terraces: A review and proposed criteria to differentiate from traditional fluvial terraces. Progress in Physical Geography 1–23.
Leeder MR and Mack GH (2001) Lateral erosion ('toecutting') of alluvial fans by axial rivers: Implications for basin analysis and architecture. Journal of the Geological Society, London 158: 885–893.
Lisenby PE and Fryirs KA (2017) Sedimentologically significant tributaries: Catchment-scale controls on sediment (dis)connectivity in the Lockyer Valley, SEQ, Australia. Earth Surface Processes and Landforms.
Martel-Cea A, Maldonado A, Grosjean M, et al. (2016) Late Holocene environmental changes as recorded in
the sediments of high Andean Laguna Chepical, Central Chile (32□S; 3050 m a.s.l.). Palaeogeography, Palaeoclimatology, Palaeoecology.
Mather AE (2006) Arid environments. In: Perry C and Taylor KG (eds) Environmental Sedimentology. Oxford: Blackwell.
Mather AE and Hartley AJ (2005) Flow events on a hyperarid alluvial fan: Quebrada Tambores, Salar de Atacama, northern Chile. In: Harvey AM, Mather AE and Stokes M (eds) Alluvial Fans: Geomorphology, Sedimentology, Dynamics. London: Geological Society of London, Special Publications, 251, 9–29.
Mather AE and Stokes M (2017) Bedrock structural control on catchment-scale connectivity and alluvial fan processes, High Atlas Mountains, Morocco. In: Ventra D and Clarke LE (eds) Geology and Geomorphology of Alluvial and Fluvial Fans: Terrestrial and Planetary Perspectives. London: Geological Society of London, Special Publications, 440.
Mather AE, Harvey AM and Stokes M (2000) Quantifying long term catchment changes of alluvial fan systems. Geological Society of America Bulletin 112: 1825–1833.
Mather AE, Stokes M and Whitfield E (2017) River terraces and alluvial fans: The case for an integrated Quaternary fluvial archive. Quaternary Science Reviews 166: 74–90.
Moreiras SM, Pont IV and Araneo D (2018) Were merely storm-landslides driven by the 2015-2016 Nin˜o in the Mendoza River valley? Landslides.

Nicoletti PG and Sorriso-Valvo M (1991) Geomorphic controls of the shape and mobility of rock avalanches. Geological Society of America Bulletin 103: 1365–1373.
Ortega C, Vargas G, Rutllant JA, et al. (2012) Major hydrological regime change along the semiarid western coast of South America during the early Holocene. Quaternary Research 78: 512–527.
Paskoff R (1977) Quaternary of Chile, et al. The state of research. Quaternary Research 8: 2–31.
Pepin E, Carretier S, Guyot J, et al. (2010) Specific suspended sediment yields of the Andean rivers of Chile and their relationship to climate, slope and vegetation. Hydrological Sciences Journal 55: 1190–1205.
Pierson TC (2005) Hyperconcentrated flow-transitional process between water flow and debris flow. In: Jakob M and Hungr O (eds) Debris-Flow Hazards and Related Phenomena. Berlin: Springer, 159–202.
Postma G (1986) Classification for sediment gravity-flow deposits based on flow conditions during sedimentation. Geology 14: 291–294.
Riebe CS, Kirchner JW and Finkel RC (2004) Sharp decrease in long-term chemical weathering rates along an altitudinal transect. Earth and Planetary Science Letters 218: 421–434.
Riebe CS, Sklar LS, Lukens CE, et al. (2015) Climate and topography control the size and flux of sediment produced on steep mountain slopes. PNAS 112(51): 15574–15579.
Riquelme R, Rojas C, Aguilar G, et al. (2011) Late Pleistocene-early Holocene paraglacial and fluvial sediment history in the Turbio Valley, semiarid Chilean Andes. Quaternary Research 5: 166–175.
Roda-Boluda D, D'Arcy M, McDonald J, et al. (2017) Lithological controls on hillslope sediment supply: Insights from landslide activity and grain size distributions. Earth Surface Processes and Landforms.
Salas I, Herrera C, Luque JA, et al. (2016) Recent climatic events controlling the hydrological and the aquifer dynamics at arid areas: The case of Huasco River watershed, northern Chile. Science of The Total Envi Sorriso-Valvo M, Antronico L and Le Pera E (1998) Controls on modern fan morphology in Calabria, Southern Italy. Geomorphology 24: 169–187.
Stokes M and Mather AM (2015) Controls on modern tributary-junction alluvial fan occurrence and morphology: High Atlas Mountains, Morocco. Geomorphology 248: 344–362.
Tiner RJ, Negrini RM, Antinao JL, et al. (2018) Geophysical and geochemical constraints on the age and paleoclimate implications of Holocene lacustrine cores from the Andes of central Chile. Journal of Quaternary Science 33(2): 150–165.

Tully CD, Rech JA, Workman TR, et al. (2019) In-stream wetland deposits, megadroughts, and cultural change in the northern Atacama Desert, Chile. Quaternary Research 91: 63–80.
Veit H (1996) Southern Westerlies during the Holocene deduced from geomorphological and Pedological Studies in the Norte Chico, Northern Chile (27-33□S). Palaeogeography, Palaeoclimatology, Palaeoecology 123: 107–119.
Wang H, Harvey AM, Xie S, et al. (2008) Tributaryjunction fans of China's Yangtze Three-Gorges valley: Morphological implications. Geomorphology 100: 131–139.
Wells SG and Harvey AM (1987) Sedimentologic and geomorphic variations in storm-generated alluvial fans, Howgill Fells, northwest England. Geological Society of America Bulletin 98: 182–198.
Wilcox AC, Escauriaza C, Agredano R, et al. (2016) An integrated analysis of the March 2015 Atacama floods. Geophysical Research Letters 43: 8035e8043.
Wilford DJ, Sakals ME, Innes JL, et al. (2004) Recognition of debris flow, debris flood and flood hazard through watershed morphometrics. Landslides 1: 61–66.
Wohl E (2017) Connectivity in rivers. Progress in Physical Geography 41: 345–362.

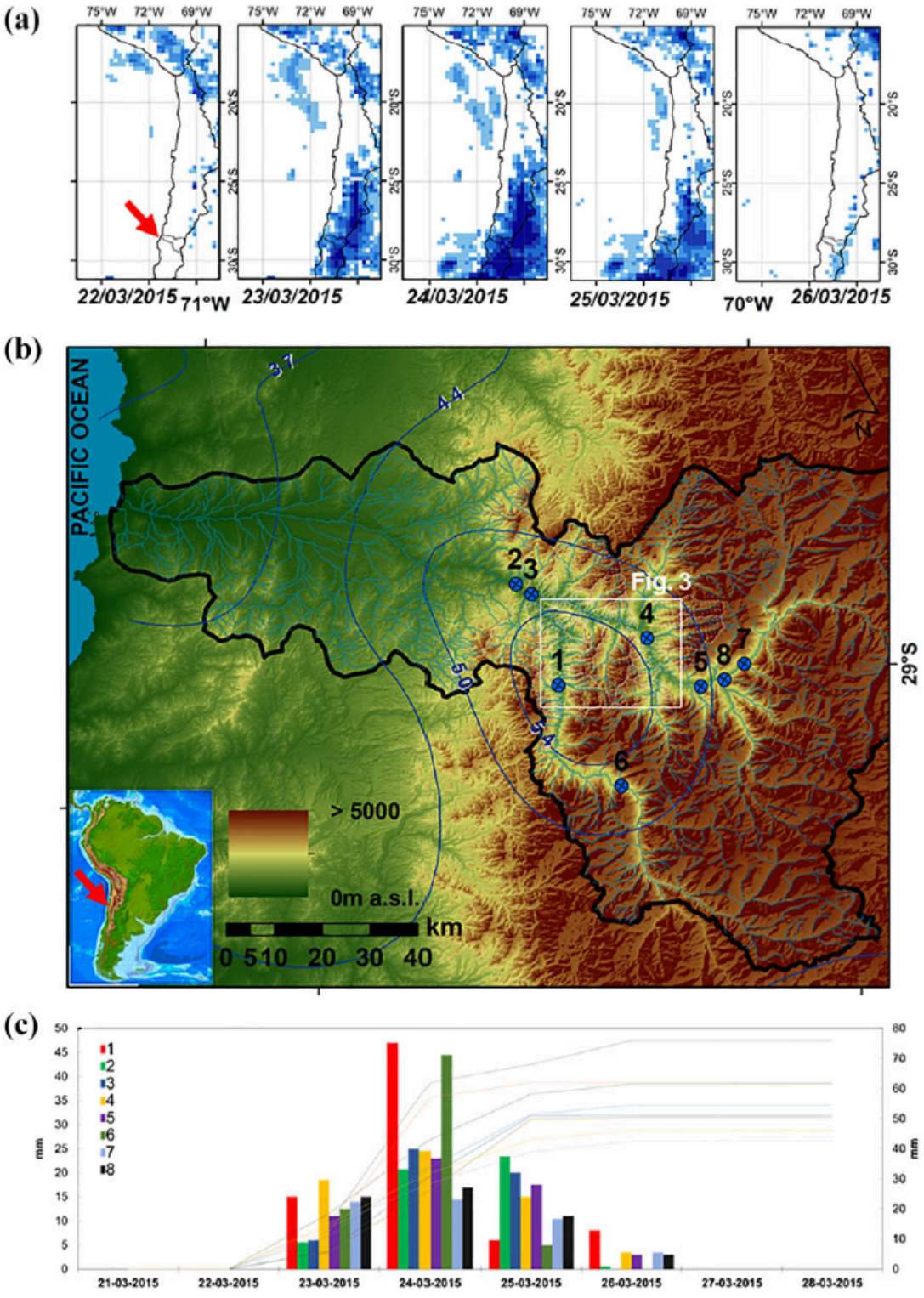

Figure 1. (a) The satellite-based spatial distribution of accumulated precipitation during 23–26 March 2015 from the Tropical Rainfall Measuring Mission 3B42 product (https://giovanni.gsfc.nasa.gov/giovanni/) for northern Chile area. Red arrow highlights the study area. (b) Shuttle Radar Topography Mission (SRTM)

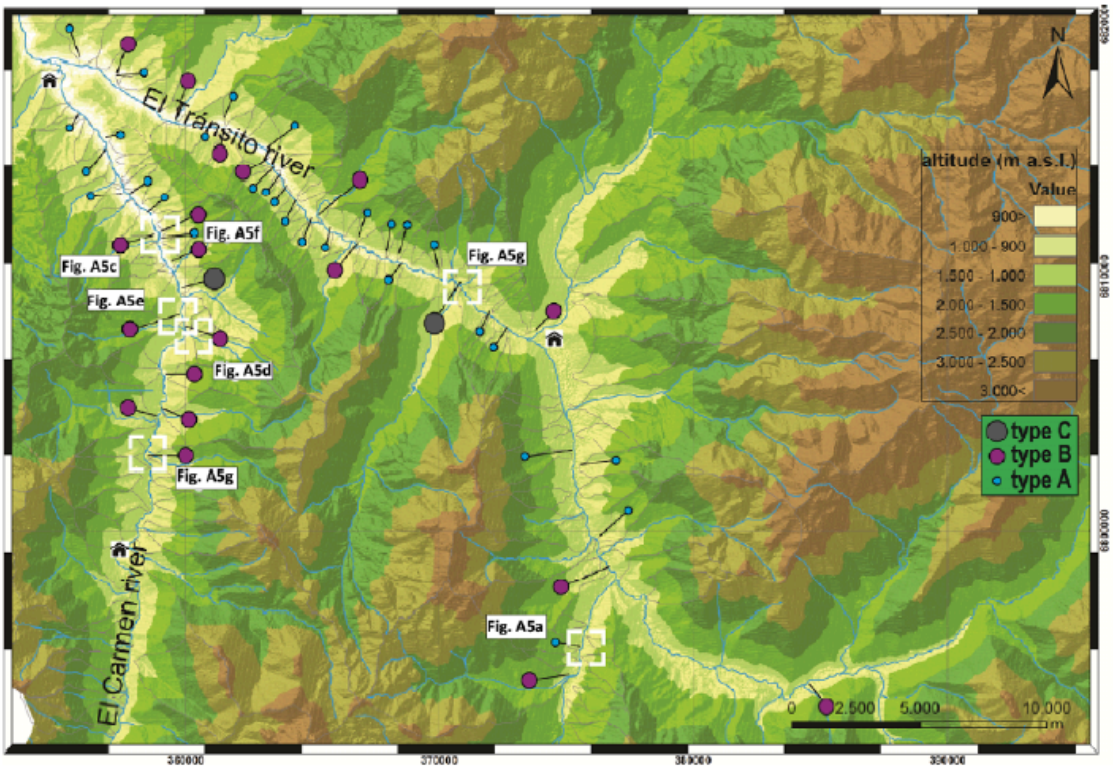

Figure 2. Situation map of fan classification from volumes of sediment. The white boxes show the location of tributary-junction alluvial fans whose facies association and geomorphic features are described in detail. The small houses represent the main towns in the area.

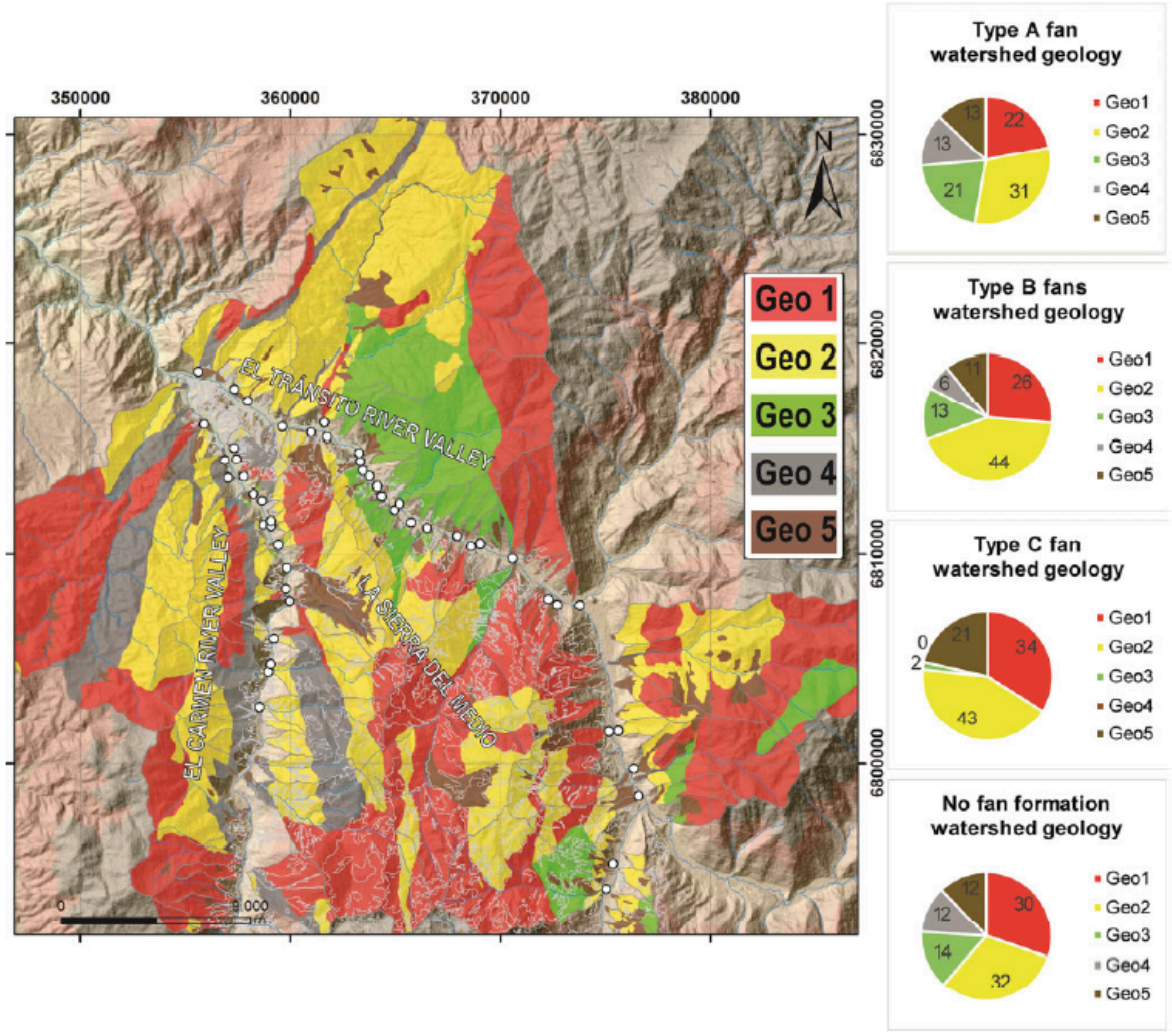

Figure 3. Geological groups (Geo1 to Geo5; geotechnical classes) and percentage of each group depending on volume of sediments delivered onto the fans. The geological groups are described in detail in supplemental Figure A2. The white dots correspond to the location of the 49 fans.

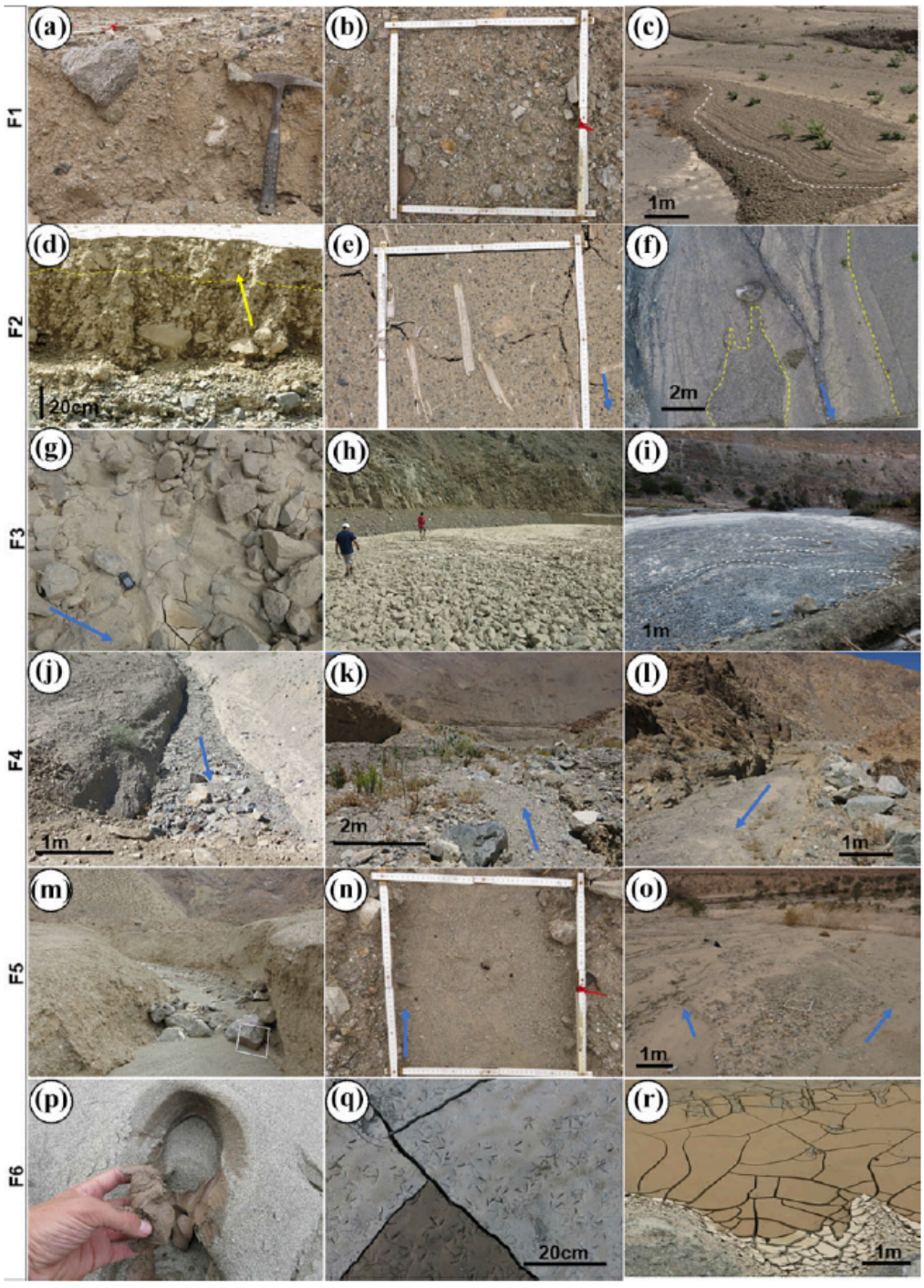

Figure 4. Photographs of facies and geomorphic features in cross-section and in ground views. Scale is indicated for each picture (quadrat is 60 cm/side; GPS is 10 cm long; hammer is 33 cm; person is ~180 cm tall); the detailed descriptions are presented in the main text. (a)–(c) Facies 1; (d)–(f) facies 2; (g)–(i) facies 3; (j)–(l) facies 4; (m)–(o) facies 5; (p)–(r) facies 6.

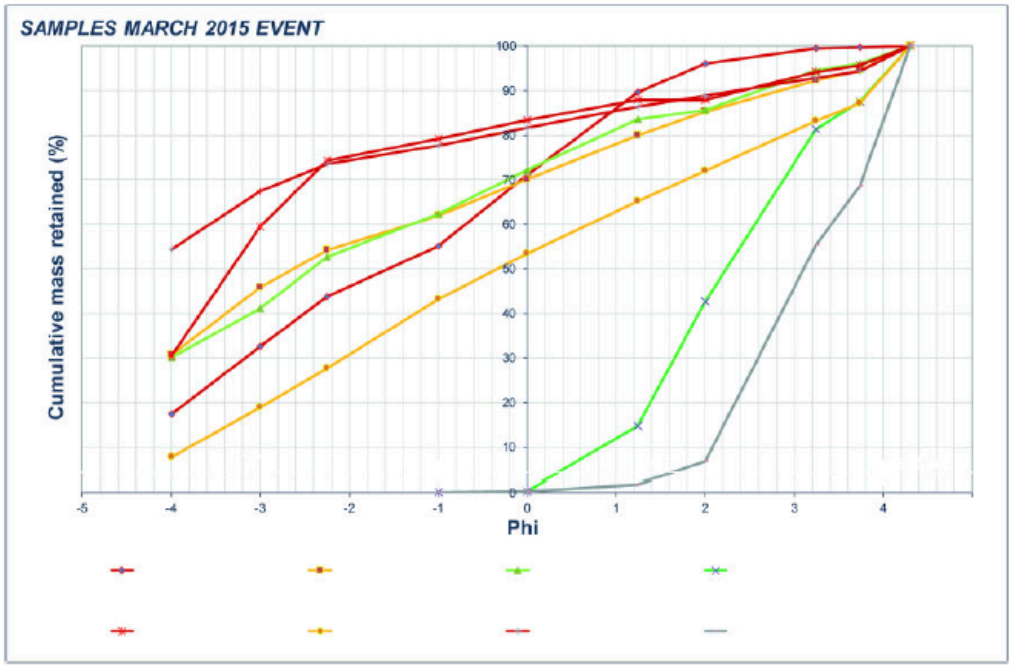

Figure 5. Granulometric distribution for sediment collected on all facies types formed after the March 2015 storm. For samples of facies 1, 2 and 3 sediments represent the matrix, whereas facies 4, 5 and 6 represent the whole sediments.

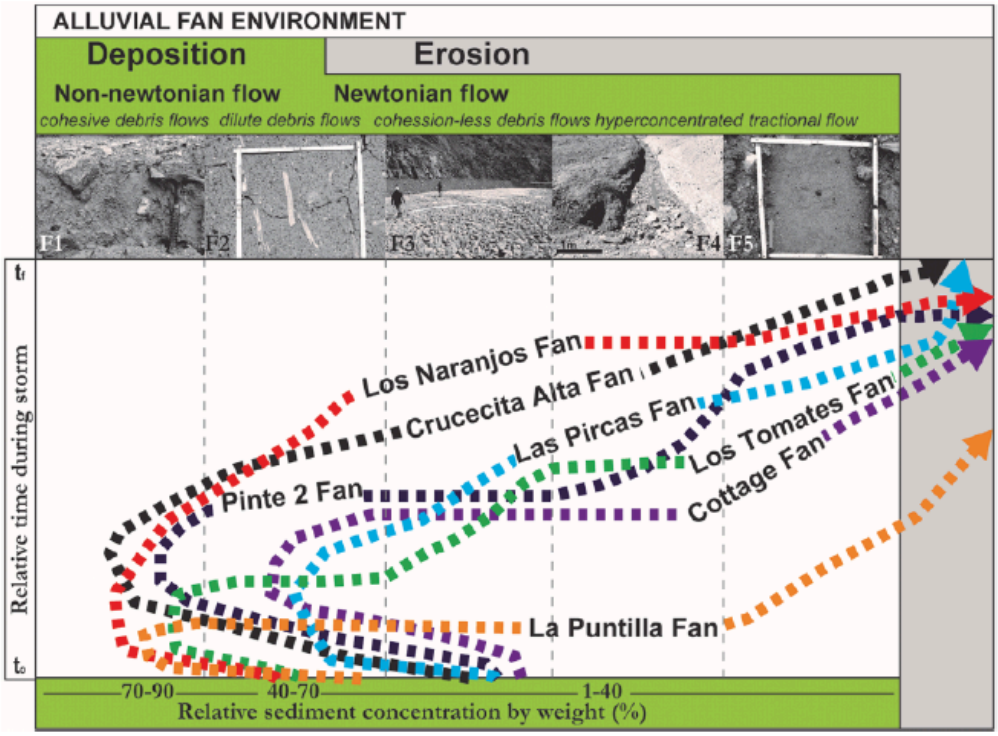

Figure 6. Conceptual model showing the changes in the relative sediment concentration by weight (%) against the relative time during the storm for the tributary-junction alluvial fan environment of representative fans of El Huasco River valley. The dashed lines represent the sequence of depositional and erosional events for the most representative fans presented, and pictures of F1 to F5 indicate the depositional archive associated with the specific time during the storm. This figure is based on the conceptual model of Wells and Harvey (1987), with emphasis on presenting the coeval behaviour of deposition and erosion.
t_o: initiation; t_f: cessation.

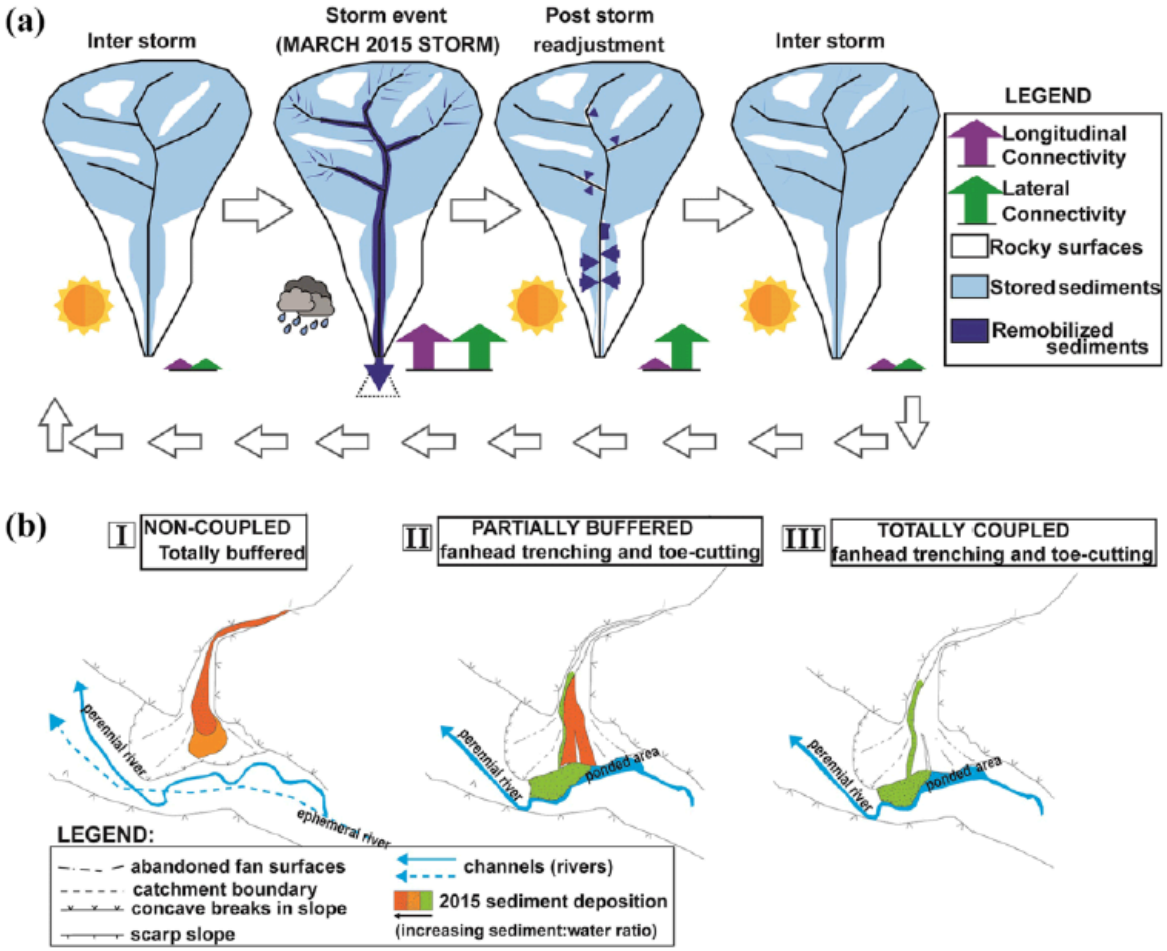

Figure 7. (a) Conceptual model of the theoretical timeline of storm-driven changes in connectivity within transport-limited catchments of fluvial valleys based on the March 2015 event field observations. Grey empty arrows at the bottom of the image indicate the direction in time. Purple and green arrow lengths indicate the relative enhancement of both lateral and longitudinal connectivity within the catchments. Dark-blue arrows within the catchments indicate remobilised sediments by different landslide processes. In post-storm readjustment, white areas in the main channels indicate the strong impact of the March 2015 event in the alluviated channels. Inter-storm configuration that follows indicates the refilling of the previously emptied channels. Field evidence is provided in supplemental Figure A9. (b) Conceptual model for the different coupling status and coupling mechanisms activated after the March 2015 event in tributary-junction alluvial fans. (I) Example of fans that do not present basally induced mechanisms that facilitate coupling for both perennial and ephemeral channels. (II) Example of fans with lateral toe-cutting that foreshortens the alluvial fan and proximally induced coupling with fan-head trenching. Buffering of sediments in the abandoned fan surfaces is related to initial surges of cohesive debris flows. (III) Example of fans with complete coupling with basally induced trenching together with fan-head trenching, facilitating sediment bypass towards the trunk valley.